Experimental validation of the modelling of surface roughness effects by an effective impedance

Olivier FAURE[1]; Benoit GAUVREAU[1]; Fabrice JUNKER[2]; Philippe LAFON[2]

[1] Ifsttar, Nantes, France

[2] EDF R&D, Clamart, France

ABSTRACT

Natural grounds can exhibit small geometry irregularities, compared to the wavelength, which are called surface roughness. Using effective impedance is a useful way to model the effects of surface roughness on outdoor sound propagation, particularly in numerical methods as it avoids the meshing of small irregularities. In this paper, firstly an effective impedance model taking into account the surface roughness spectrum of the ground is exposed. Secondly, an experimental campaign of sound pressure measurements above 1/10 scale 2D rough surfaces is presented. The same profile characterized by a gaussian roughness spectrum is designed in two polystyrene boards coated with resin. One board is felt-covered to simulate an absorbing rough surface and the other is left uncovered to simulate a reflective rough surface. Finally, the experimental results are compared to analytical calculations with the effective impedances corresponding to the two experimental rough surfaces, respectively. Those results show good agreement, thus validating the effective impedance approach and allowing more accurate SPL predictions for future impact studies in environmental acoustics.

Keywords: Ground roughness, effective impedance I-INCE Classification of Subjects Number(s): 24.9
(See `http://www.inceusa.org/links/Subj%20Class%20-%20Formatted.pdf`.)

1. INTRODUCTION

In the field of outdoor sound propagation, rough grounds are often encountered. Surface roughness is defined as small geometry irregularities compared to the wavelength. The roughness can be natural or artificial (cultivated soils). Effective impedance models for ground roughness take into account the effects of roughness on sound propagation by considering the rough surface as a flat surface with a modified impedance condition. The use of an effective impedance could be useful in numerical methods, particularly in time-domain methods such as FDTD or Transmission Line Matrix, as it avoids the meshing of the smaller roughness elements and reduces computation times (1, 2). Recently, an effective impedance approach was used to model rough sea surfaces in order to study numerically the propagation of noise generated by offshore wind farms (3).

The effective impedance boss model considers a deterministic rough profile formed by scatterers of constant shape. It allows to calculate an effective impedance function of the geometry of the scatterers (4). Heuristic extensions of this model have been validated by reduced scale laboratory experiments (5, 6, 7) and outdoor measurements over agricultural surfaces such as plowed grounds (8).

Surface roughness may be known statistically. Another effective impedance formulation obtained from electromagnetics studies accounts for the effects of a random surface on wave propagation. Refered as the Small Perturbation Method (SPM) model, it expresses the effective impedance function of the roughness spectrum of the surface. This paper presents the model and a reduced-scale laboratory measurement campaign over reflective and absorbing rough surfaces, which are defined by a gaussian roughness spectrum. These measurements are carried out in order to validate the SPM model for sound propagation. In the first section, the effective impedance model is exposed. The second section describes the surfaces over which measurements are made and details the experimental set-up. The results are analyzed in the third section, showing the effects of roughness on sound pressure levels and comparing the measurements with analytical solutions using the effective impedance model.

[1] olivier.faure@ifsttar.fr

2. THE SPM EFFECTIVE IMPEDANCE MODEL

2.1 Model formulation

Bourlier *et al.* exposed an effective impedance model for electromagnetic waves propagation above a rough surface (9). This model is obtained using the Small Perturbation Method (SPM). A 2D "low variying" rough surface is considered with $|k_0\zeta\cos(\theta)| < 1$ et $|\partial\zeta/\partial x| < 1$, as shown on figure 1 where $k_0 = 2\pi f/c_0$ is the wave vector in air, c_0 the sound speed in the air, $\zeta(x)$ is the height profile, θ the angle of incidence, Z_0 the characteristic impedance of the air and Z_S the impedance of the surface.

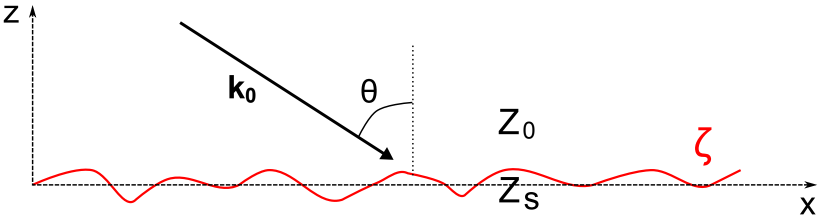

Figure 1 – Wave vector $\mathbf{k_0}$ incident to a rough surface ζ

It is thus possible to perform finite expansions of the Green's function for a point source and the Neumann boundary condition. Then the field above the rough surface can be modeled with a boundary integral formulation. A mean value of this integral is calculated using the Dyson equation and the Feynman diagram formalism (10). Finally after some manipulations (9, 11), it is possible to obtain a plane-wave reflection coefficient and an effective impedance for the rough surface. This effective impedance is function of the roughness spectrum W of the surface. This roughness spectrum is defined as the Fourier Transform of the autocorrelation function of the surface height profile ζ (or spectral density of ζ). The effective impedance accounts for the mean effect of the random roughness on the wave propagation. This reasoning can be applied to the acoustics equations which are similar to the ones considered in electromagnetism. The mean effect on sound propagation of a 2D acoustically hard (Neumann boundary condition) rough surface is modeled by the following effective admittance :

$$\beta_R = \int_{-\infty}^{+\infty} \frac{d\kappa'}{k_0 k_z} \left(k_0^2 - \kappa\kappa'\right) W(\kappa - \kappa') \tag{1}$$

with $k_z^2 = k_0^2 - \kappa^2$, $\kappa = k_0 \sin(\theta)$ and W the roughness spectrum of the surface. The equation (1) has a pole p for $k_z(p) = 0$. A reformulation is possible in order to remove the pole and facilitate the numerical integration (9).

For an absorbing surface, the effect of roughness is taken into account as a correction of the surface admittance $\beta_S = 1/Z_S$:

$$\beta_{eff} = \beta_S + \beta_R \tag{2}$$

2.2 Comparison with the boss model

The SPM effective impedance model is supposed to be valid for every height profile ζ and roughness spectrum W. The boss effective impedance model, based on Twersky's work (12), allows to calculate an effective admittance for a roughness formed by cylindrical scatterers (figure 2). For propagation normal to the scatterers ($\phi = 0$) and grazing incidence ($\theta = \pi/2$) it is defined as (8) :

$$\beta_{eff} = \beta_S - ik_0 V\left[\delta - 1 + \gamma\Omega\right] \tag{3}$$

with γ the specific heat ratio, Ω the porosity of the ground, V the cross-sectional scatterer area per unit length. The parameter δ is given by $\delta = 2s_2/v_2$ with $s_2 = (1/2)(1+K)$, $v_2 = 1 + (2\pi V s_2/3b)$. K is a hydrodynamic factor depending of the scatterer shape (values of K for different shapes are given in (4)).

In order to show the equivalence between the two effective impedance models for a deterministic roughness, a profile of hard close-packed cylinders (β=0, Ω=0) of radius $a = 0.09$ m and mean spacing $b = 0.1$ m is considered. On one hand, these geometrical properties are used to calculate an effective impedance with the equation (3). On the other hand, the roughness spectrum of this profile is calculated and the equation (1) is numerically integrated in order to obtain an other effective impedance. The effective impedances obtained by the two different models are compared on figure 3. Despite some oscillations due to the numerical integration and a non-zero real part above 800Hz for the SPM model, figure 3 shows that the two models give equivalent results.

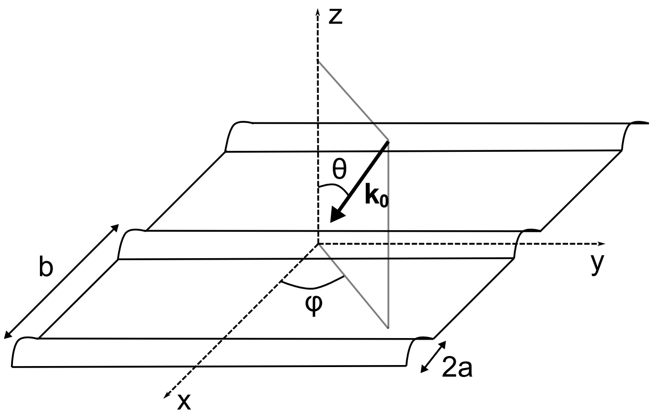

Figure 2 – Wave vector $\mathbf{k_0}$ incident to a surface containing cylinders of radius a and mean center-to-center spacing b (4).

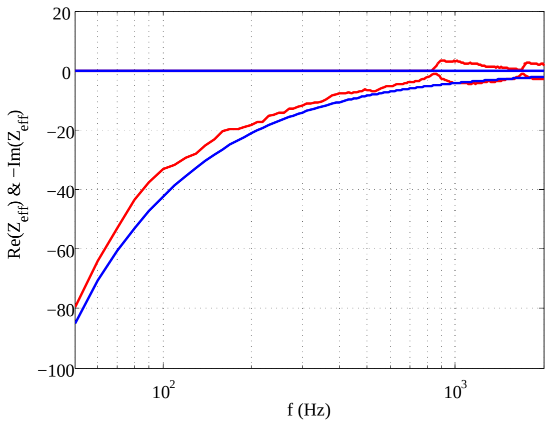

Figure 3 – Real part and imaginary part of the effective impedances calculated with (—) the SPM model and (—) the boss model for a rough profile composed of small cylinders.

3. EXPERIMENTAL SET-UP

3.1 Experimental rough surfaces

Measurements are performed in order to validate the SPM model for a rough surface with a gaussian spectrum for middle-range propagation. A gaussian spectrum is defined in k-space by :

$$W(k) = \frac{\sigma_h^2 l_c}{2\sqrt{\pi}} e^{\frac{-k^2 l_c^2}{4}} \tag{4}$$

wtih σ_h is the standard-deviation of the height and l_c the correlation length (13). If the roughness spectrum of a profile is supposed to be gaussian, the roughness is then defined statistically by the two parameters σ_h and l_c.

A 55 m bidimensional rough surface defined by gaussian spectrum with by $\sigma_h = 0.05$ m and $l_c = 0.2$ m is cut at 1/10 scale into two polystyrene boards. The dimension of the boards is 6 m x 1.8 m (each board is actually composed of 3x3 smaller boards of dimension 2 m x 0.6 m). The width was determined by Fresnel zone calculations (14), in order to minimise edge effects. The boards are coated with epoxy resin in order to make them reflective. One surface is left uncovered in order to leave it reflective (figure 4(a)). The other one is covered with felt of thickness 1 mm to make it absorbing (figure 4(b)). Two perfectly flat boards of the same dimensions are also considered, one being only coated with epoxy resin and the other being resin-coated and covered with felt. Measurements above the flat boards are carried out to characterize the effect of roughness compared to the perfectly flat ground case.

3.2 Measurements configuration

Measurement of impulse reponse functions above the four surfaces (reflective rough, absorbing rough, reflective flat, and absorbing flat) are performed, as shown on figure 5(a) for the absorbing rough surface. The source is a 3/4" tweeter Clarion SRH292HX (frequency response 2kHz-120kHz). The receiver is a 1/4" B&K 4961 multi-field microphone (frequency range 5Hz-20kHz). The signal emitted is a white-noise and

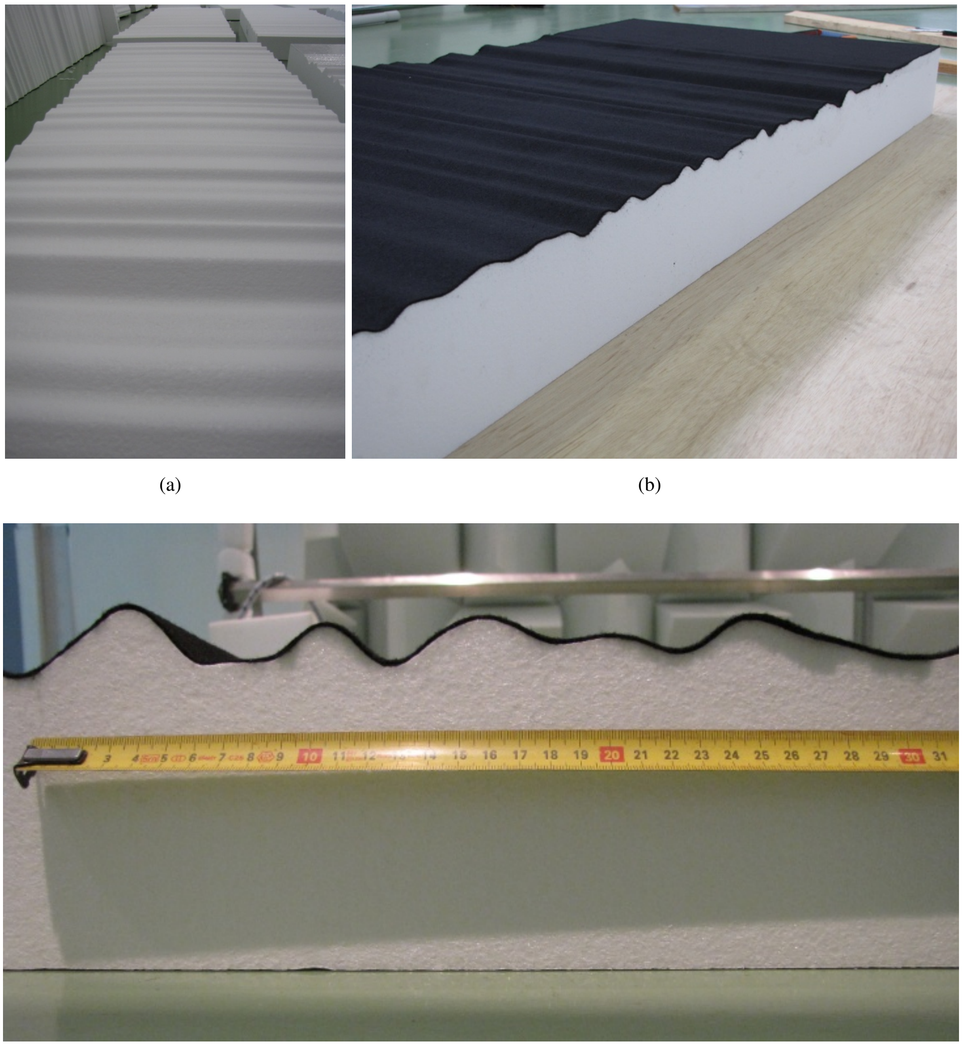

(a) (b)

(c)

Figure 4 – Experimental rough surfaces characterised by a gaussian spectrum. (a) Coated with expoxy resin; (b) Coated with expoxy resin and covered with felt; (c) Roughness scale.

the impulse responses are obtained using the B&K PULSE LabShop software. Six source heights H_S are considered : 0.02 m, 0.1 m, 0.2 m, 0.3 m, 0.4 m and 0.5 m. The microphone position is controlled by an automatic displacement system (figure 5). For each source height, the measurements are made at 5 microphone heights H_R : 0.1 m, 0.2 m, 0.3 m, 0.4 m, 0.5 m and at 39 distances d : 1.7 m, 1.8 m, … 5.4 m, 5.5 m. Thus for each of the four surfaces 1170 impulse responses are measured.

These measurements are done at 1/10 scale compared to an outdoor sound propagation case. Due to the properties of the source and the microphone, the frequency range of validity is 2kHz-20kHz. At real scale, the measurement geometries exposed earlier are multiplied by 10 and range of validity thus becomes 200Hz-2000Hz.

3.3 Impedance measurements

As shown by equation (2), the effective impedance formulation requires to know the impedance Z of the flat surfaces, in particular the absorbing felt-covered surface. Nevertheless it is found that the surface only coated with expoxy resin are not actually perflectly reflective, so its impedance is also measured. Impedance properties are estimated with *in-situ* measurements by a two-microphone technique (15, 16) and considering the Miki impedance model (17). The source is located at height $H_S = 0.6$ m. The sound levels are measured at two microphones vertically spaced above the absorbing surface, both located at a distance $d = 4$ m from the source and at heights $H_{R1} = 0.6$ m and $H_{R2} = 0$ m (the second microphone is put on the ground). The measured sound level difference $\Delta L = L_{R1} - L_{R2}$ between the two microphones is compared to an analytical solution of propagation above a flat impedant ground, obtained with the Weyl-Van Der Pol formula (14). Miki

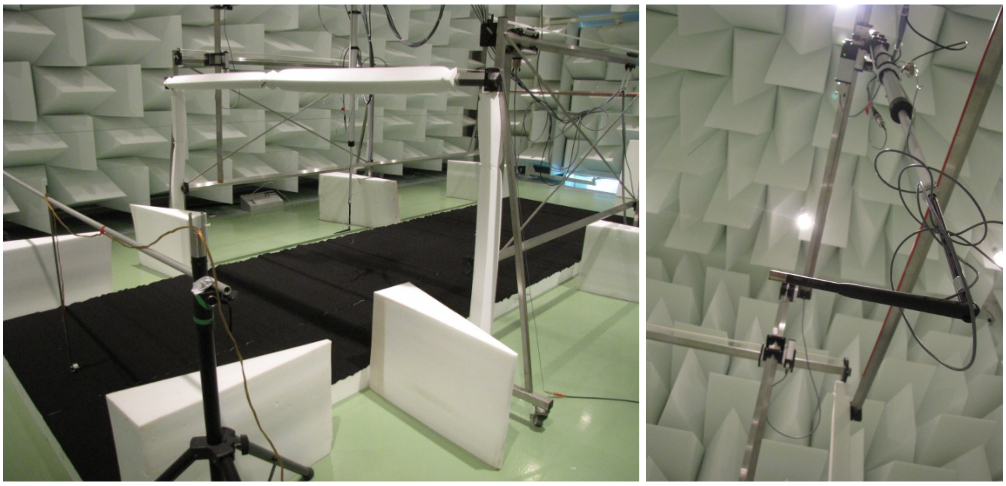

(a) (b)

Figure 5 – (a) Global view of the measurement configuration; (b) Zoom on the microphone controlled by the automatic displacement system.

ground impedance model is given by (17) :

$$k_M = \frac{\omega}{c_0}\left(1 + 7.81\left(\frac{f}{\sigma}\right)^{-0.618} + i11.41\left(\frac{f}{\sigma}\right)^{-0.618}\right) \tag{5a}$$

$$Z_M = Z_0\left(1 + 5.50\left(\frac{f}{\sigma}\right)^{-0.632} + i8.43\left(\frac{f}{\sigma}\right)^{-0.632}\right) \tag{5b}$$

with σ the air flow resistivity of the ground expressed in kN.s.m^{-4}. The impedance is corrected as follows to model an hard backed layer of thickness e (14) :

$$Z_S = Z_M \coth(-ike) \tag{6}$$

The two parameters σ and e are estimated by minimising the difference between the measurement and the analytical solution. This impedance measurement procedure is applied on the perflecty flat boards, with the geometry reproduced at reduced scale. The results at full scale are shown on figure 6. The resin-coated surface is found to have a flow resistivity of 10000 kN.s.m^{-4} and an infinite thickness. The felt-covered surface is found to have a flow resistivity of 380 kN.s.m^{-4} and a thickness of 0.01 m, which corresponds to the properties of a grassy ground. For the latter, one can note that at reduced scale this thickness value coincides with the real thickness of the felt layer (1 mm).

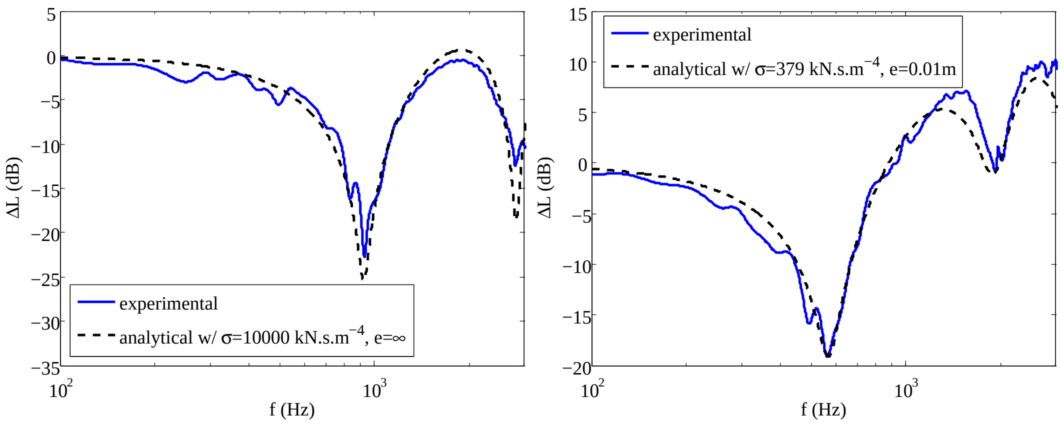

Figure 6 – Estimation of the impedance of the flat boards at full scale. (left) Epoxy resin-coated surface; (right) Epoxy resin-coated and felt-covered surface.

3.4 Estimation of the source power spectrum

The power spectrum of the source is estimated in order to express the sound pressure levels relative to the source power. Impulse response measurements are performed above the floor of the semi-anechoic room at distances $d = 1.7$ m, 1.8 m, ... 5.4 m, 5.5 m with the source and microphone at the same height $H_S = H_R = 0.6$ m. This height ensure a clear separation between the direct and floor-reflected signals. At each one of the 39 measurement points, the signal is windowed in order to keep only the direct signal and the source power spectrum L_S is evaluated as :

$$L_S = L_{exp}(d) - L_{th}(d) \tag{7}$$

where L_{exp} is the measured sound pressure level spectrum for the direct field and L_{th} the analytical solution given by $20\log(e^{ikd}/d)$. The source power spectrum considered in the rest of this paper to express "SPL relative to the source spectrum" is the mean value of all these evaluations, represented at full scale on figure 7.

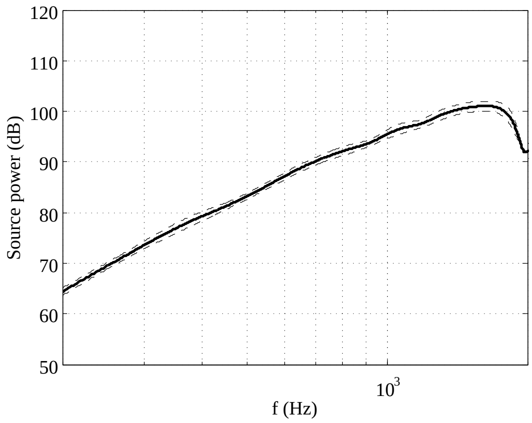

Figure 7 – Estimation of the source power spectrum : (—) mean value; (- -) mean value ± one standard-deviation

4. RESULTS COMPARISONS

The sound pressure levels relative to the source power are assessed experimentally and analytically at each point above each surface. From now on, the dimensions and frequency are considered for full scale. In this section the results are exposed for the case with the source at $H_S = 2$ m above the ground as a representative example. The SPL measured above the rough boards are compared to the SPL measured above the perflecty flat boards (in order to characterize the roughness effects) and to analytical solutions using the SPM effective impedance model. The effective impedance are computed using equation (2), with the gaussian roughness spectrum given by equation (4) and the impedance of the flat surfaces estimated with the Miki model.

4.1 Reflective surfaces

SPL mappings over the reflective surfaces are represented on figure 8. Comparing the measurements over the flat (upper mapping) and rough surfaces (center mapping) shows that the roughness globally reduces the sound level, particularly at the larger distances near the ground for the lower frequencies (e.g. 200 and 500 Hz). The propagation over the rough surface leads to the formation of more disturbed interference patterns. The SPL estimated analytically using the effective impedance model (lower mapping) are in good accordance with the measurements, and the global shapes of the modified interference patterns are also correctly observed.

The spectra at different measurements positions are drawn in figure 9. The grounds dips are the destructive interferences due to the interaction between the direct and the reflected field. For all measurements, a strong shift of the main ground dip towards the lower frequencies due to the roughness is seen. This leads the SPL measured above the rough surface (blue curve) to be significantly lower than over the flat ground (black curve) for the lower frequencies. At grazing incidence, further from the source ($d = 45, 55$ m) and closer to the ground ($H_R = 1$ m), the SPL are strongly reduced up to 1000 Hz, with for example a reduction of about 10 dB between 300 and 700 Hz at $d = 55$ m. The SPL predicted analytically using the effective impedance model (red curves) are generally in good accordance with the measurement above the rough hard surface. At $H_R = 3$ m, the position of the main and second ground dip are correctly predicted. One can notice that the spectra measured above the rough surface shows some oscillations, due to the multiple reflections induced by the roughness. These reflections are not taken into account by the effective impedance model.

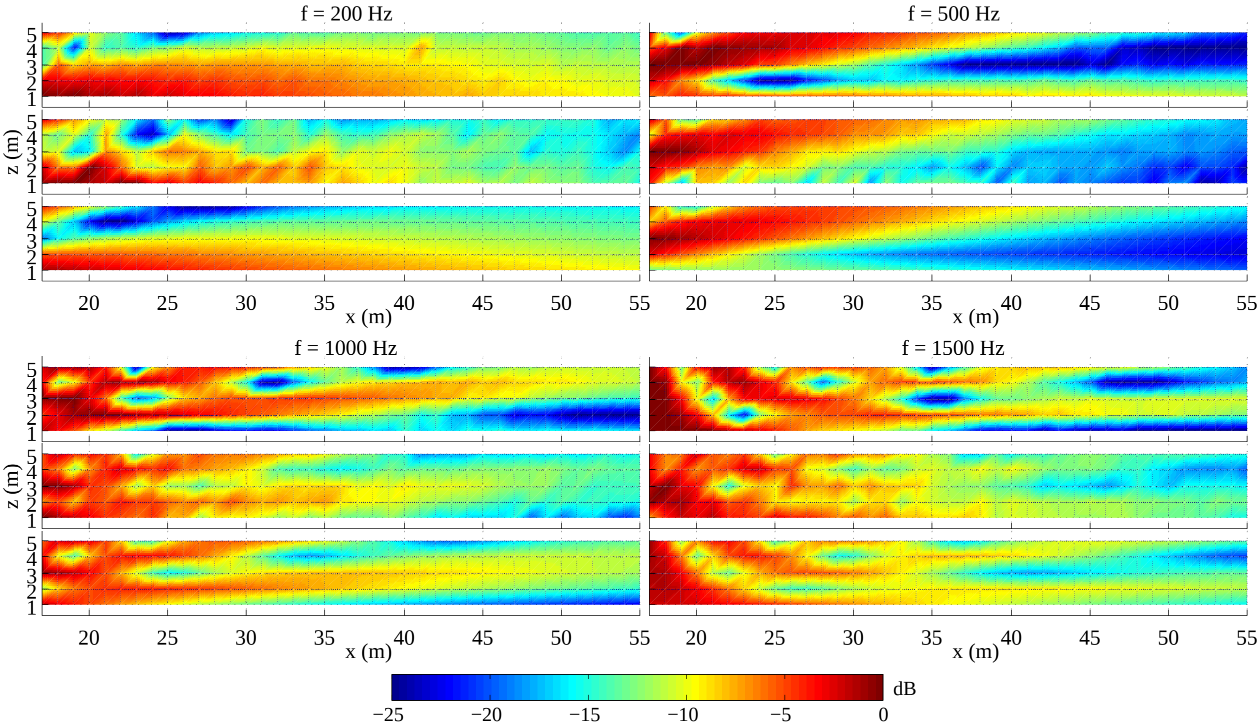

Figure 8 – Source located at $H_S = 2$ m above the reflective surfaces : for $f = 200$, 500, 1000 and 1500 Hz, mapping of (up) the measured SPL above the flat ground, (center) the measured SPL above the rough ground, (down) the analytical result with the effective impedance model.

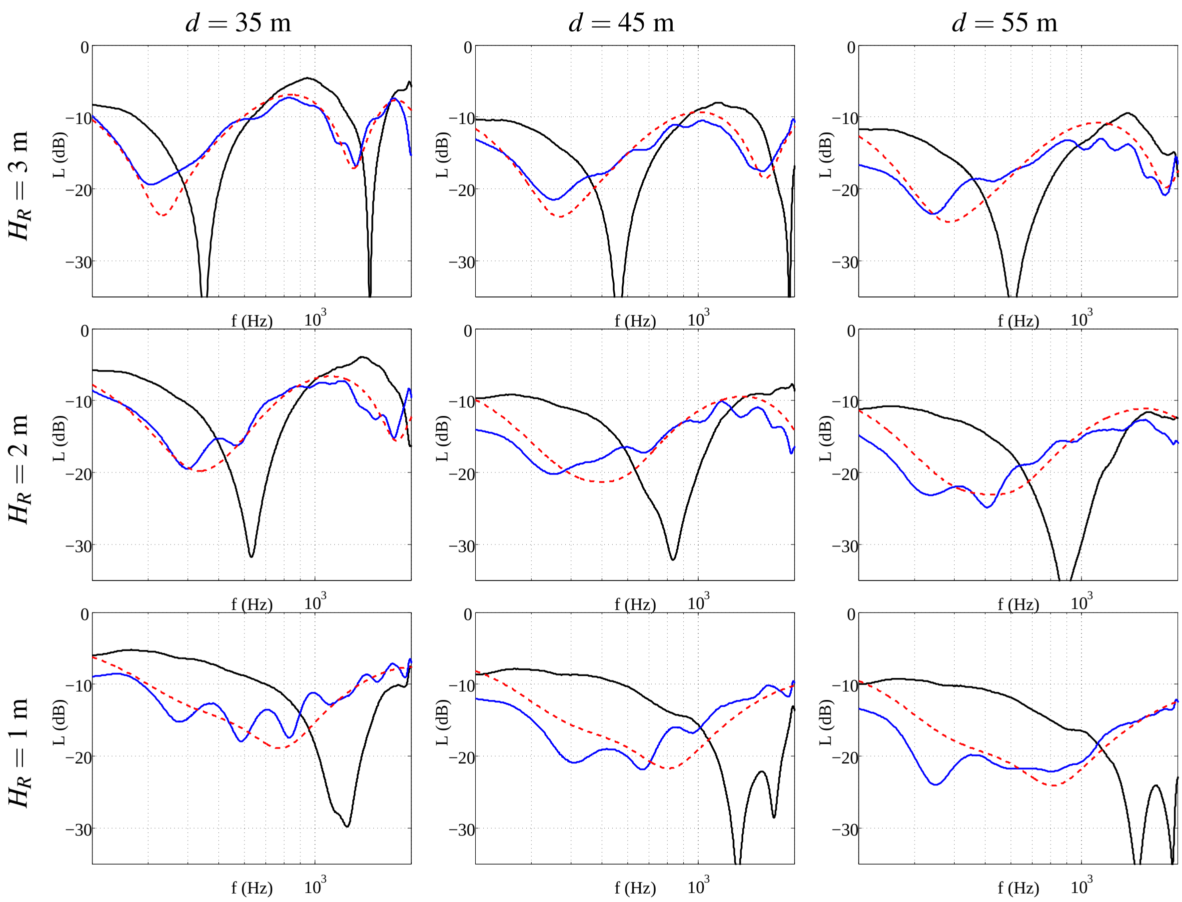

Figure 9 – SPL at different positions over the reflective surfaces for $H_S = 2$ m : (—) measurement over the flat surface, (—) measurement over the rough surface, (- -) analytical solution with effective impedance.

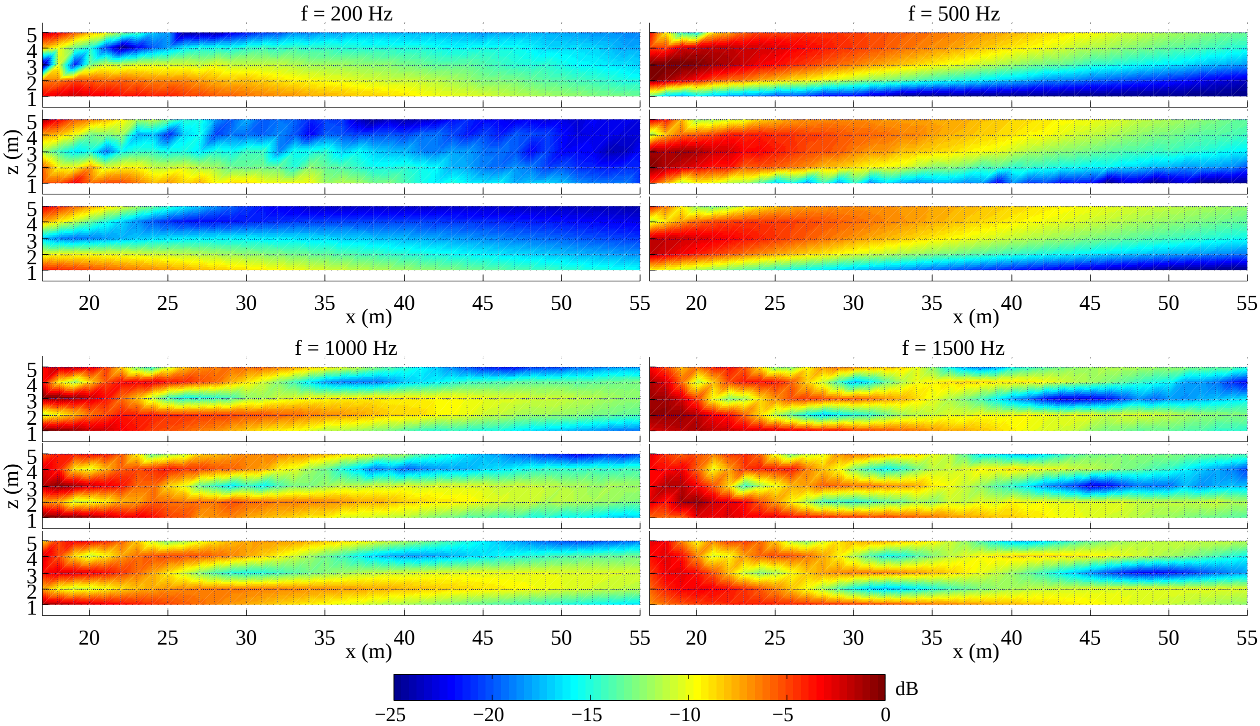

Figure 10 – Source located at $H_S = 2$ m above the absorbing surfaces : for $f = 200$, 500, 1000 and 1500 Hz, mapping of (up) the measured SPL above the flat ground, (center) the measured SPL above the rough ground, (down) the analytical result with the effective impedance model.

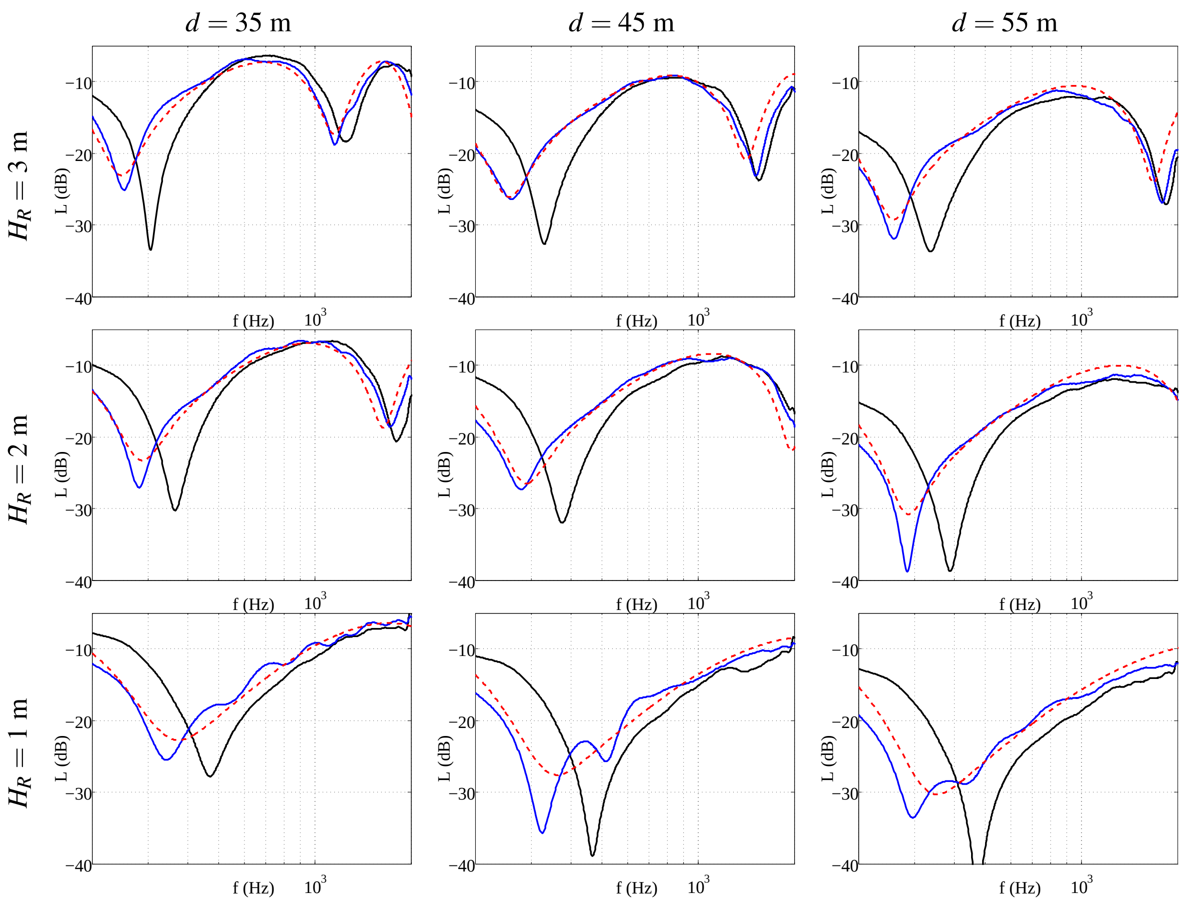

Figure 11 – SPL at different positions over the absorbing surfaces for $H_S = 2$ m : (—) measurement over the flat surface, (—) measurement over the rough surface, (- -) analytical solution with effective impedance.

4.2 Absorbing surfaces

SPL mappings over the absorbing surfaces are shown on figure 10. The effect of roughness is less pronounced compared to the previous case with reflective surfaces. At 200 Hz, the SPL relative to the source power above the rough absorbing surface is reduced at larger distances (over $d = 35$ m). At the other frequencies, the main noticeable effect of the roughness is a small spatial shift in the position of the interference patterns. Nevertheless these effects are quite well taken into account by the analytical SPL (lower mappings). However, these analytical solutions are obtained considering an effective impedance calculated with $\sigma = 380$ kN.s.m^{-4} and an infinite thickness for the flat surface impedance, whereas a finite thickness of $e = 0.01$ m was found by the impedance measurement in section 3.3. Indeed, the analytical results are less in accordance with the measurements if this value of e is considered.

The spectra for the absorbing surfaces are drawn on figure 11. As with the reflective case, the roughness induces a shift of the ground dip in the low frequencies (blue curve). The ground dip of the perflecty flat absorbing surface (black curve) being at lower frequencies than for the flat reflective surface, the roughness effect is less pronounced compared to the reflective surfaces case, but still significant at low frequencies. Closer to the ground at $H_R = 1$ m the level is reduced by more than 10 dB at 300 Hz. At higher frequencies, above 1000 Hz, the effect of roughness is nearly negligible, as the black and blue curve superimpose. The SPL calculated with the effective impedance model (red curves) show again a good agreement with the measurement over the rough surface.

5. CONCLUSIONS

An effective impedance model for rough surfaces has been exposed. The SPM model is function of the roughness spectrum of the surface and allows to characterize the effects of a random rough surface on sound levels as a correction of the surface admittance. An experimental measurement campaign was performed to validate this model for propagation over rough surfaces with a gaussian spectrum, statistically defined by two parameters (the height standard deviation and the correlation length). Measurements of impulse responses were performed at scale 1/10 up to a distance of 55 m, above a reflective rough surface coated with epoxy resin and a more absorbing rough surface coated with epoxy resin and covered with felt. The measurements were also performed above two flat surfaces, one made reflective and the other made absorbing in the same way. The impedances of the flat surfaces were measured by a two-microphone technique in order to calculate the effective impedance of the rough surfaces. The results show qualitatively and quantitatively the significant effect of the considered roughness on the sound pressure levels. For the absorbing surface, which at full scale has impedance properties similar to a grassy ground, the effect of the roughness can be important at the lower frequencies. The analytical solutions using the effective impedance model are in good agreement with the measurements above the rough surfaces. This shows the SPM effective impedance approach would be an efficient method to take into account the effects of random ground roughness for future impact studies in environmental acoustics.

ACKNOWLEDGEMENTS

This work was carried out within the context of a PhD Thesis, partnership between Ifsttar (Nantes, France) and EDF R&D (Clamart, France). The authors thank Keith Attenborough for the discussions and the invitation to present this paper, and Christophe Bourlier for his help and time.

REFERENCES

1. Faure O, Gauvreau B, Junker F, Lafon P. Effective impedance models for rough surfaces in time-domain propagation methods. In: Proceedings of Inter-noise 2013. Innsbruck, Austria; 2013. .

2. Faure O, Benoit B, Junker F, Lafon P. Modélisation de sols irréguliers par une impédance effective: application aux méthodes temporelles. In: Proceedings of the 12th french acoustical congress. Poitiers, France; 2014. .

3. Van Renterghem T, Botteldooren D, Dekoninck L. Airborne sound propagation over sea during offshore wind farm piling. The Journal of the Acoustical Society of America. 2014;135(2):599–609.

4. Boulanger P, Attenborough K, Taherzadeh S, Waters-Fuller T, Li KM. Ground effect over hard rough surfaces. The Journal of the Acoustical Society of America. 1998;104(3):1474–1482.

5. Chambers JP, Sabatier JM. Recent advances in utilizing acoustics to study surface roughness in agricultural surfaces. Applied Acoustics. 2002;63(7):795–812.

6. Boulanger P, Attenborough K. Effective impedance spectra for predicting rough sea effects on atmospheric impulsive sounds. The Journal of the Acoustical Society of America. 2005;117(2):751–762.

7. Bashir I, Taherzadeh S, Attenborough K. Diffraction assisted rough ground effect: Models and data. The Journal of the Acoustical Society of America. 2013;133(3):1281–1292.

8. Attenborough K, Waters-Fuller T. Effective impedance of rough porous ground surfaces. The Journal of the Acoustical Society of America. 2000;108(3):949–956.

9. Brelet Y, Bourlier C. SPM numerical results from an effective surface impedance for a one-dimensional perfectly-conducting rough sea surface. Progress in Electromagnetics Research-pier. 2008;PIER 81:413–436.

10. Bass FG, Fuks IM. Wave scattering from statistically rough surfaces. Oxford Pergamon Press International Series on Natural Philosophy. 1979;93.

11. Brelet Y. Diffusion des ondes électromagnétiques par une surface rugueuse monodimensionnelle sous incidences modérées et rasantes: application au domaine maritime. Nantes; 2008.

12. Lucas RJ, Twersky V. Coherent response to a point source irradiating a rough plane. The Journal of the Acoustical Society of America. 1984;76(6):1847–1863.

13. Bourlier C, Pinel N, Kubické G. Method of Moments for 2D Scattering Problems: Basic Concepts and Applications. Wiley ed.;.

14. Attenborough K, Li KM, Horoshenkov K. Predicting Outdoor Sound. Taylor & Francis; 2006.

15. Bérengier M, Garai M. A state-of-the-art of in-situ measurement of the sound absorption coefficient of road pavements. Rome, Italia; 2001. .

16. Carpinello S, L'hermite P, Berengier M, Licitra G. A new method to measure the acoustic surface impedance outdoors. Radiation Protection Dosimetry. 2004;111(4):363–367.

17. Miki Y. Acoustical Properties of porous materials : Modifications of Delany-Bazley models. Journal of the Acoustical Society of Japan (E). 1990;11(1):19–24.